JOURNAL OF CATALYSIS 89, 217–225 (1984)

Measurement of the Morphology of High Surface Area Solids: Effect of Network Structure on the Simulation of Porosimetry

WM. CURTIS CONNER AND ALAN M. LANE

Department of Chemical Engineering, The University of Massachusetts, Amherst, Massachusetts 01003

Received January 25, 1984; revised May 18, 1984

A computer simulation of mercury porosimetry based on a pore/throat network model is tested for the effects of changing various structural parameters. These include lattice size, connectivity, and the shape of the pore and throat size distributions. Some general rules of thumb are presented for simplifying the interpretation of porosimetry data.

INTRODUCTION

Mercury porosimetry has become a common method for measuring catalyst pore size distributions. However, the proper interpretation of the data has been disputed ever since the development of the technique by Ritter and Drake in 1945 (*1*). A parallel capillary tube model is used in the conventional interpretation. The pore structure model, consisting of cylindrical, nonintersecting tubes passing through the solid, is well-recognized as an oversimplification and is inadequate in describing pore structure.

In a previous paper we presented a pore/throat network model with which to interpret the data (*2*). The model, shown in Fig. 1, represented the pore structure as relatively large voids (pores) interconnected by smaller constrictions (throats). The model was used to analyze experimental results on compacted fumed silicas. Also, a computer simulation of the porosimetry process based on this model was able to reproduce the experimental results. Using this model, two significant improvements over the more conventional parallel capillary tube model were demonstrated.

(1) By assigning intrusion to penetration of the throats and extrusion to evacuation of the pores, both the pore and throat size distributions (PSD and TSD) are obtained.

(2) By viewing porosimetry as a network process, we found that there is a considerable difference between the void size distributions measured by porosimetry and that which actually exists in the catalyst. We learned that this results from the sequential nature of intrusion/extrusion through a network structure.

The computer simulations results were obtained by using a simple cubic network with a $7 \times 7 \times 7$ lattice size, a connectivity of six, and a normal distribution of pore and throat sizes. This network construction is used as a base case in this study. In addition, we examine some of the consequences of using other pore structures on porosimetry measurements. Because the shifts between measured and actual pore and throat size distributions are caused by the network structure, it is expected that these shifts depend on the type of network used and the size distributions examined. To test this expectation, we specifically study the lattice size, lattice geometry, and shape of the TSD and PSD.

These studies indicate a rather complex set of relationships among porous structures and their measurement by porosimetry. However, this seemingly inextricably complex situation is made manageable by the suggestion of some simple rules to use when interpreting porosimetry data.

EXPERIMENTAL

Details of our computer simulation of the

0021-9517/84 $3.00
Copyright © 1984 by Academic Press, Inc.
All rights of reproduction in any form reserved.

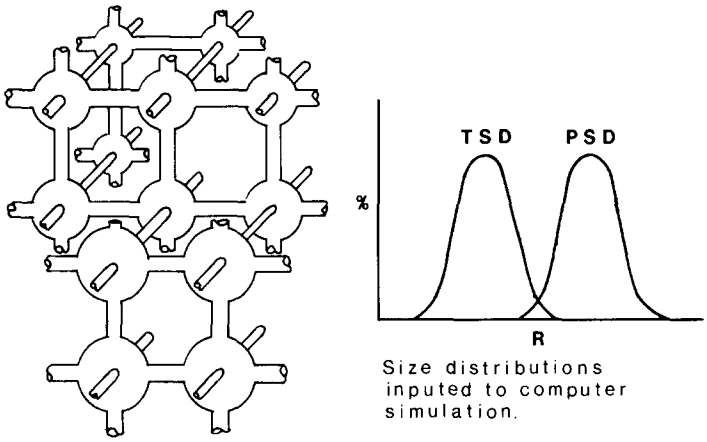

FIG. 1. Three-dimensional pore/throat network. Throat and pore sizes assigned at random from a normal distribution.

porosimetry process have been presented elsewhere (*3*). The network shown in Fig. 1 is a simple cubic lattice of size 3 × 3 × 3 with a connectivity of six. However, the network can be constructed to reflect any size distribution and geometric arrangement of pores and throats. In fact, the central concern of this study involves the dependence of porosimetry measurements on different network constructions. Pore and throat sizes are assigned randomly to the network from distributions and are the only input parameters in the simulation. Once the network has been constructed, it can be subjected to the conditions expected to occur during intrusion and extrusion. In this study, only the construction of the pore/throat network is changed and not the simulation of the porosimetry process.

Lattice size is changed by merely increasing or decreasing the dimensions of the network. In addition to the base case, we study 5 × 5 × 5 and 9 × 9 × 9 lattices.

Lattice geometry is primarily examined by changing the connectivity. The network in Fig. 2B is modified by adding another diagonal set of throats, as depicted in Fig. 2A, which gives a connectivity of 8. The connectivity is varied by randomly removing ¼ and ½ of the throats from the network with a connectivity of 8 to achieve connectivities of 6 and 4, respectively. In this case, the pores actually exhibit some distribution of connectivities around a mean value.

Various distributions of sizes are assigned to the throats and pores. In addition to the base case normal distribution, the width is varied and the shape is skewed to the large or small pore sizes.

RESULTS

The results of these simulations are presented in Figs. 3–6. For each simulation three graphs are shown representing the pressure/volume (*P/V*) data, TSD, and PSD. The general characteristics of these curves will be presented in this section. The effect of changes in various network parameters (as mentioned above) will be discussed in the next section.

The distribution depicted in Figs. 3–6 are based on the number frequency normalized to the numerically most abundant size (actual or measured). The other distribution curves are expressed relative to the size that is the most absorbant and abundant. The figures represent the sizes counted in the simulations. For the throat sizes in particular, the actual volume intruded is dependent on the pore connected to the intruded throat and, as will be seen, only a fraction of the throats are measured during intrusion (i.e., there are numerically more throats than pores in an interconnected net-

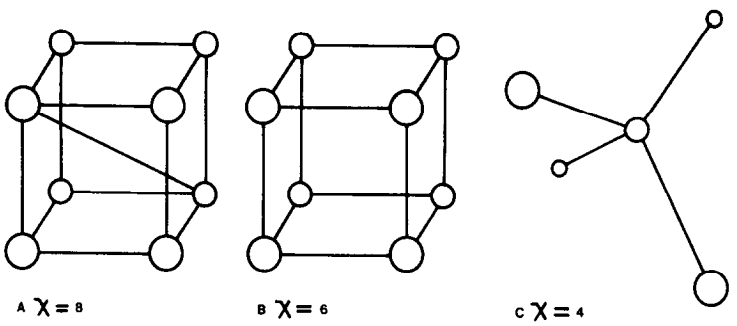

FIG. 2. Construction of lattices with varying connectivity. Shown are connectivities of eight ($x = 8$), six ($x = 6$), and four ($x = 4$).

work.) For these reasons the integrated numerical area of penetrated or measured sizes is not constant, whereas, the total intruded or extruded volume is the same for throats and pores in these simulations.

The simulated pressure/volume graphs are shown in Figs. 3a–6a. They exhibit three key characteristics of porosimetry: an "S"-shaped intrusion curve, hysteresis of extrusion, and mercury retention after the completion of extrusion. The hysteresis is caused by the different controlling geometries of the intrusion and extrusion processes, the TSD controls the intrusion and the PSD control the extrusion. Some mercury is permanently retained because individual or groups of pores become isolated from the receding mercury front during extrusion and become stranded in the network.

The throat size distributions, TDS's are shown in Figs. 3b–6b. The "ACTUAL" curve represents the TSD inputed to the simulation. The "PENETRATED" curve represents the throats which were used to access the pores. It is important to realize that only one throat per pore is needed to access the whole pore structure. With a connectivity of six, this represents only about $\frac{1}{3}$ of the throats. Equally important is the fact that the mercury takes the easiest possible route to the interior of the network (i.e., the largest penetratable throats). Therefore, only the largest third of the throats are used for access to the pores and are therefore measured. We call this phenomenon "nonlinkage" which is a network effect. Some of these throats, however, are "shadowed" because they are not accessible until a smaller throat to which they are connected has been filled. Hence, they are measured at too high a pressure. "Shadowing" (a network effect) shifts the measurement of the penetrated throats towards smaller radii, resulting in the "MEASURED" curve. This corresponds to the number, rather than volume, derivative of the intrusion curve.

The Pore Size Distributions, PSD's, are shown in Figs. 3c–6c. The "ACTUAL" curve represents the PSD inputed to the simulation. Network phenomena also shift the measurement of the pores as shown by the "MEASURED" curve (see Ref. (2)). This corresponds to the number derivative of the extrusion curve. Also shown is the distribution of stranded pores which are identified as "STRANDED."

The mean values of the simulated courses are shown in Table 1. Various ratios of these mean values are presented in Table 2. The ratio of the measured values to the actual values (P_m/P_a and T_m/T_a) indicate the magnitude of the shift caused by network effects. Shown also are the measured pore to throat size ratios (P/T) which seem to be strongly affected by the type of network examined.

DISCUSSION

In this section, we examine the effect of lattice size, connectivity, and shape of the

TABLE 1

Mean Radius (and Standard Deviation) of the Simulated Porosimetry Curves in Figs. 3–6

Lattice size, Fig. 3		ACT	MEAS	PEN/STR
5^3	*T*	128 (53)	173 (37)	179 (40)
	P	507 (177)	531 (146)	740 (49)
7^3	*T*	122 (51)	165 (34)	172 (40)
	P	483 (181)	491 (140)	739 (82)
9^3	*T*	124 (52)	164 (34)	172 (39)
	P	491 (194)	506 (135)	733 (100)
11^3	*T*	124 (53)	164 (34)	174 (40)
	P	494 (197)	509 (123)	735 (109)
Interconnectivity, Fig. 4				
= 4	*T*	131 (55)	160 (40)	170 (44)
	P	518 (194)	618 (139)	646 (212)
= 6	*T*	130 (56)	176 (37)	183 (41)
	P	518 (194)	570 (138)	778 (95)
= 8	*T*	130 (56)	184 (38)	189 (41)
	P	518 (194)	543 (149)	791 (89)
Distribution, Fig. 5				
Wide	*T*	122 (51)	165 (34)	172 (40)
	P	483 (181)	491 (140)	739 (82)
Narrow	*T*	126 (28)	149 (18)	153 (20)
	P	501 (98)	517 (68)	633 (43)
Distribution, Fig. 6.				
Skew left	*T*	106 (30)	131 (18)	140 (20)
	P	419 (149)	425 (110)	618 (96)
Normal	*T*	124 (25)	146 (13)	152 (16)
	P	498 (129)	522 (92)	656 (50)
Skew right	*T*	145 (29)	169 (12)	174 (13)
	P	589 (148)	632 (76)	750 (44)

Note. ACT = Actual, MEAS = Measured, PEN/STR = Penetrated (Throats, T), or Stranded (Pores, P).

pore and shape of the throat size distributions on the porosimetry measurements. Also, we discuss the relevance of the specific modification of the simulation in representing real physical situations.

Lattice Size

Lattice size is an important parameter in percolation type processes such as mercury porosimetry. The ratio of the number of surface pores to the number of interior pores is a surprisingly large number but decreases as the lattice size increases. The exterior pores always have direct access to the bulk mercury and therefore essentially behave as independent domains. As a result, we would expect that small lattices exhibit less sensitivity to network effects than large lattices.

The small lattice sizes examined here do not seem representative of the very large lattice sizes expected to occur in many catalyst pellets. Nonetheless, they seem to accurately reflect the typical shapes of porosimetry curves. The theoretical intrusion curves calculated for very large lattices (see Ref. (*4*), Fig. 2) exhibit a steepness that is rarely seen in porosimetry. We suspect that this is due to large pores, cracks, and fissures which divide the catalyst pellet into independent domains of smaller networks similar to the lattice size studied here.

TABLE 2

Ratios of Mean Values[a]

Lattice size, Fig. 3	P_m/T_m	P_m/P_a	T_m/T_a	T_p/T_m
5^3	3.07	1.048	1.350	1.036
7^3	2.98	1.016	1.350	1.042
9^3	3.09	1.031	1.321	1.052
11^3	3.11	1.030	1.315	1.061
Interconnectivity, Fig. 4				
= 4	3.75	1.156	1.142	1.051
= 6	3.17	1.070	1.338	1.045
= 8	3.04	1.089	1.431	1.023
Distribution, Fig. 5				
Wide	3.17	1.070	1.338	1.045
Narrow	3.47	1.030	1.179	1.023
Distribution, Fig. 6				
Skew left	3.25	1.015	1.237	1.069
Normal	3.58	1.047	1.173	1.042
Skew right	3.73	1.073	1.172	1.025

[a] P_m/T_m = Measured Pores/Measured Throats, P_m/P_a = Measured Pores/Actual Pores, T_m/T_a = Measured Throats/Actual Throats, T_p/T_m = Penetrated Throats/Measured Throats.

The effects of changing the lattice size are shown in Fig. 3. The most noticeable effect appears to be in the percentage of retained mercury in the P/V data (Fig. 3a). We can understand this effect by noting that as the lattice size increases, so does the average path length from a pore to the exterior. Therefore, there will be a greater probability that the path will be blocked by a discontinuity of mercury through which the mercury cannot extrude. Lattice size does not seem to have a major effect on the difference between measured and actual pore and throat sizes, as is seen by inspecting Figs. 3b and c and Tables 1 and 2. This is surprising because many of these ratios reflect shifts caused by network effects and should be lattice size-dependent. For this type of process, apparently other factors such as connectivity and size distributions have a greater effect.

Connectivity

Lattice geometry includes both the geometric relationship of the pores to each other and the number of connections between pores. It has been shown that percolation through networks with identical connectivities is not sensitive to the geometry (*5*). Therefore, we will emphasize the connectivity.

The connectivity of a porous structure is a fundamental characteristic of its geometry. Large (nonconcave) particles may tend to be close-packed and, therefore, at a minimum have a tetrahedral void structure with a connectivity of four. In our previous paper we studied the porosimetry of small fumed silica particles (= 100 Å diameter). These tended to pack in a way similar to a simple cubic packing with an interconnectivity of six. Asymmetric particles such as needle-like structures may pack in a more irregular fashion and have higher connectivity.

The effects of changing the connectivity are shown in Fig. 4. As connectivity increases, more potential routes are available for extrusion, causing a decrease in retained volume as observed in Fig. 4a.

The TSD in Fig. 4b show that the measured distribution shifts toward larger radii as connectivity increases. This shift occurs because a smaller percentage of the throats have to be penetrated to access the pores. The area under the measured TSD in comparison to the actual TSD also reflects this fact. For instance, for an connectivity of 8,

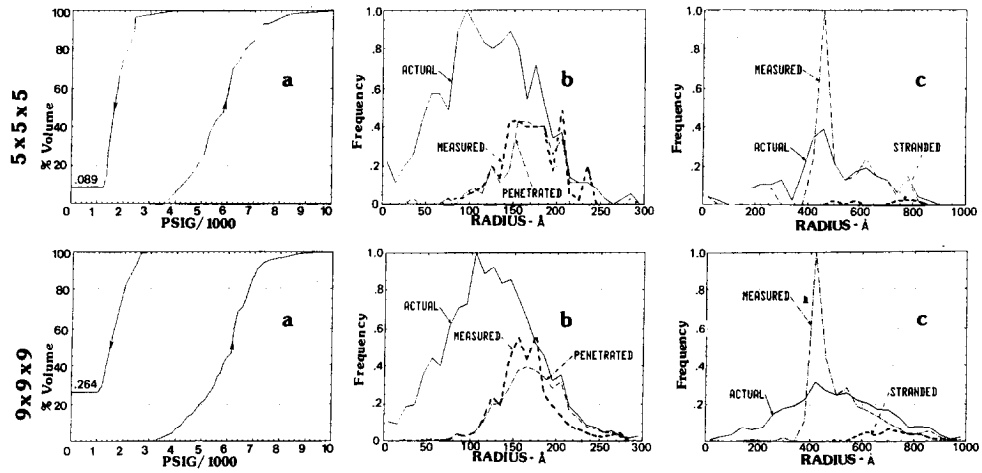

FIG. 3. (a, b, and c) Effect of various lattice sizes (5^3, and 9^3) on the Intrusion/Extrusion Curves (pressure vs volume in (a)). Also the number distribution of throat sizes (b) and the number distribution of pore sizes (c) that would result from these curves.

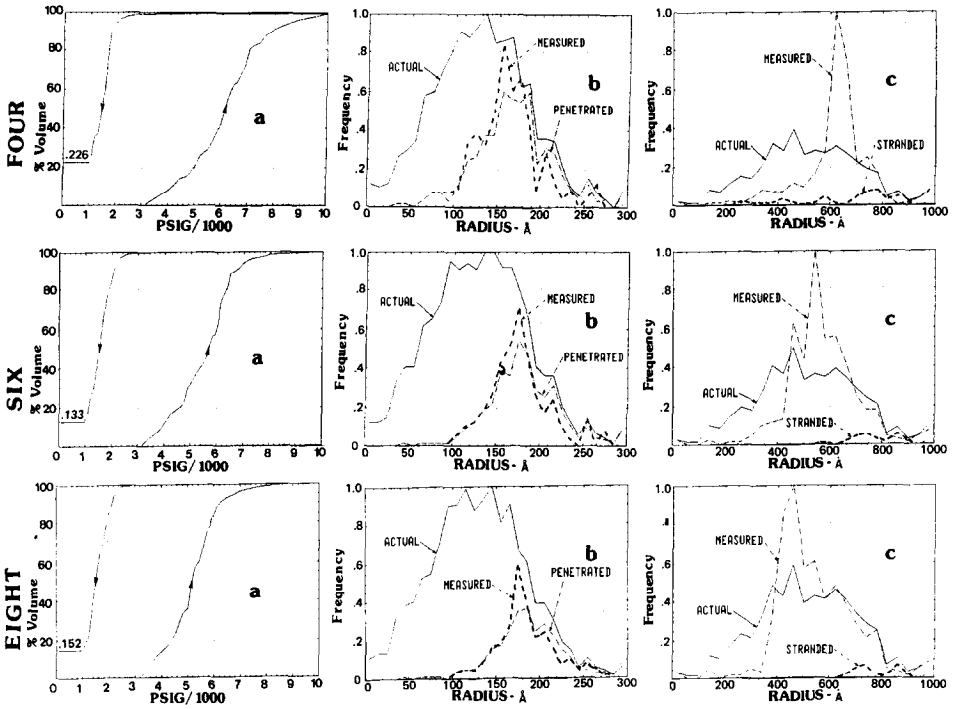

FIG. 4. (a, b, and c) Effect of various connectivities (4, 6, and 8) on the Intrusion/Extrusion Curves (pressure vs volume in (a)). Also, the number distribution of throat sizes (b) and the number distribution of pore sizes (c) that would result from these curves.

only 25% of the throats are measured. Therefore, the area ratio of the actual to measured distributions is 4.

The PSD in Fig. 4c show a sizeable decrease in the shift of the measured distribution toward smaller radii as connectivity increases. As the throat to pore number ratio increases, there is more potential for finding empty throats adjacent to a pore from which to recede. As a result, more pores are able to evacuate at the proper pressure.

These shifts are large enough to speculate about their use as an analytical tool. Note that the measured PSD and TSD Shift in opposite directions as connectivity is change. As seen in Table 2, therefore, the pore to throat size ratio is a strong function of the connectivity. This suggests the possibility that, with further analysis, the pore-to-throat size ratio and the mercury retention could be used to ascertain the connectivity of a catalyst pellet (*6*).

Size Distribution

Pore and throat size distributions are the intended objects of measurement of porosimetry. Although a normal Gaussian distribution was used in our previous study, any shape of the distribution of pore and throat sizes should be possible in a catalyst pellet. For instance, some natural systems seem to have log-normal distributions (skewed toward smaller sizes) (*7*). The distribution should be a direct consequence of the type of solid particles and the amount of compaction. For instance, an agglomerate of monodispersed particles should display a narrow distribution.

Figure 5 shows the effect of changing the width of the PSD and TSD. As the distribution is made narrower, the amount of retention decreases. Moreover, as expected, the intrusion and extrusion curves are wider for wider distributions. This also effects a

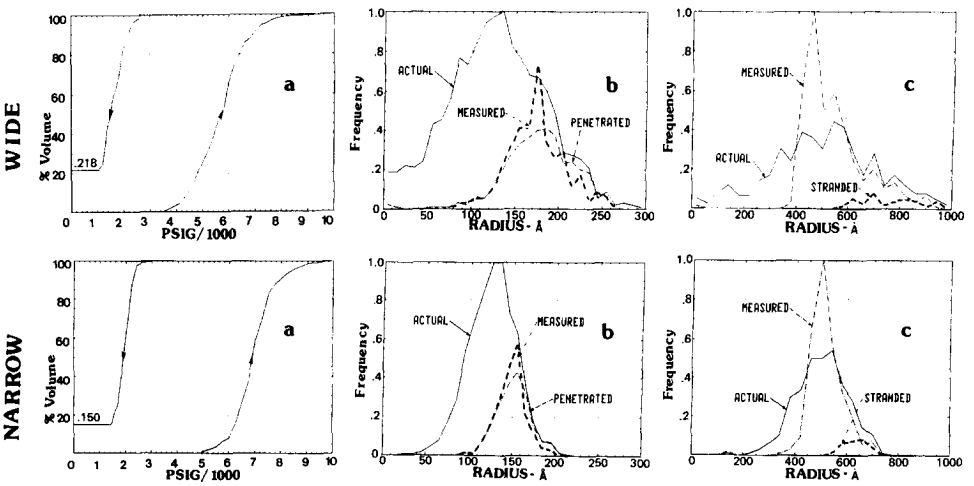

FIG. 5. (a, b, c) Effect of the distribution of sizes (width) on the Intrusion/Extrusion Curves (pressure vs volume in (a)). Also, the number distribution of throat sizes (b) and the number distribution of pore sizes (c) that would result from these curves.

larger shift between the measured and actual TSD and PSD for the wider distribution.

Figure 5 shows the effect of changing the width of the PSD and TSD. As the distribution is made narrower, the amount of retention decreases. Moreover, as expected, the intrusion and extrusion curves are wider for wider distributions. This also effects a larger shift between the measured and actual TSD and PSD for the wider distribution.

Distributions skewed toward large radii are designated "skewed left" and toward small radii are "skewed right." The effects of changing the shape of the size distributions are seen in Fig. 6. The retention is significantly higher for size distributions skewed left. A potential explanation for this can be understood by studying the PSD.

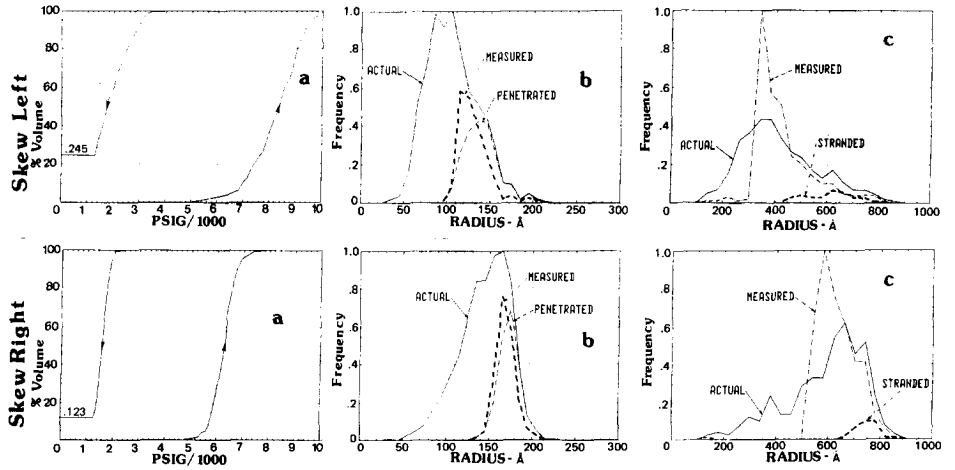

FIG. 6. (a, b, and c) Effect of skewing TSD and PSD from small (left) to large (right) radii on the Intrusion/Extrusion Curves (pressure vs volume in (a)). Also, the number distribution of throat sizes (b) and the number distribution of pore sizes (c) that would result from these curves.

The most likely pores to be stranded tend to be the largest ones; they are the last to be evacuated. When the PSD is skewed left, these larger pores are relatively well-distributed in the lattice and therefore have a greater probability of becoming isolated during the extrusion process. However, percolation theory predicts a specific retention for a given lattice structure (*8, 9*). The distribution of pore and throat sizes, providing they are statistically random, should have no effect on the amount of retention. Therefore the exact nature of the increased retention is not well understood.

Another dramatic change is the steeper slopes of the intrusion and extrusion curves when the shapes of the size distributions are changed from skewed left to skewed right. The measured TSD adheres to the right-hand side (RHS) of the actual TSD (representing the large throats). If the RHS is spread out as in the skewed left distribution, so also will the measured TSD be spread out along with the intrusion curve. Conversely, if the RHS of the actual TSD is steep as with the skewed-right distribution, the measured TSD will be narrow and the intrusion curve will be steep.

A similar line of reasoning explains the behavior of the extrusion curve. The measured PSD always rises steeply on the left-hand side (LHS) of the actual PSD due to the "shadowing" phenomena. It then follows the RHS of the actual PSD fairly closely; there is however a slight shift due to the stranded pores. If the RHS is spread out then the extrusion curve will also be broadened. If the RHS is steep, then the extrusion curve will also be steep.

A General Rule of Thumb

Examination of these various network structures has developed a more complete understanding of the relationship of a porous structure and its measurement by porosimetry. However, the various trends tend to be somewhat weak (with possible exceptions such as connectivity) and overlap in many cases. Without an *a priori* knowledge of the pore structure, application of these trends in the interpretation of actual porosimetry data would be ambiguous at best.

However, two general trends can be quite useful and easily applied in interpreting the data. The first trend is that the shift in the measurement of the PSD is usually not very large. Therefore, assignment of the derivative of the extrusion curve to the PSD *as it stands* seems to be a reasonable approximation.

A second trend is that the measured TSD always seems to adhere to the RHS of the actual TSD and mimic its general shape. This means that the measured distribution closely reflects the distribution of the largest throats. It would be reasonable to broaden the measured TSD of real porosi-

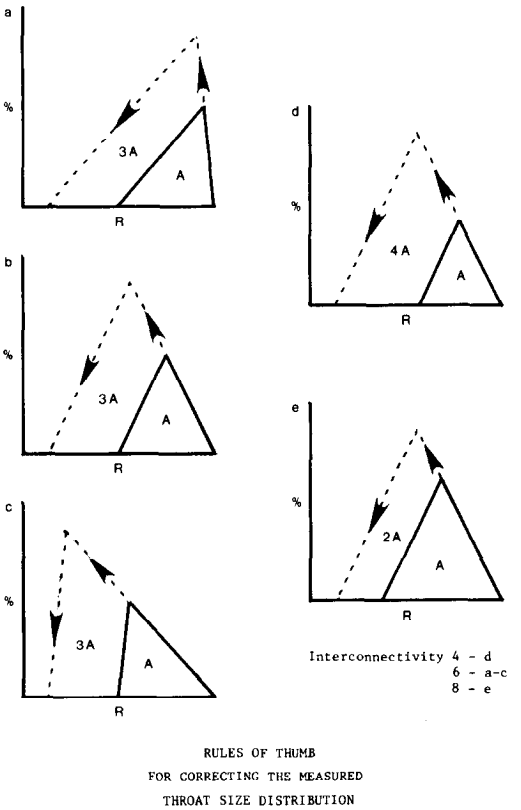

FIG. 7. Rules of thumb for correcting the measured throat size distribution to relate the measured to the actual distribution of effective throat dimensions.

metry data toward smaller radii in such a way that the area of the actual TSD is three times the area of the measured TSD (or a factor of $X/2$ for a different connectivity). Also, the actual TSD should have the same general shape as the measured TSD. This process is demonstrated in Fig. 7 for some different types of measured TSD. This should be a reasonable approximation of the actual TSD in the catalyst under analysis.

CONCLUSION

In this study we have related various structural parameters of porous materials to their measurement by mercury porosimetry. Because of the complexity of the various relationships, application of this insight to actual porosimetry data without *a priori* knowledge of the porous structure would be difficult. Therefore, some general rules of thumb have been proposed with which porosimetry data can be interpreted to obtain a more realistic approximation of the actual PSD and TSD in the catalyst being measured.

ACKNOWLEDGMENTS

The authors gratefully acknowledge the financial support of Gulf Research and Development. The National Science Foundation is thanked for their donation of the mercury porosimeter.

REFERENCES

1. Ritter, H. L., and Drake, L. C., *Ind. Eng. Chem.* **17,** 782 (1945).
2. Conner, Wm. C., Lane, A. M., Ng, K. M., and Goldblatt, M. J., *J. Catal.* **83,** 336 (1983).
3. Lane, A. M., Ph.D. dissertation, University of Massachusetts, 1983.
4. Larson, R. G., and Morrow, N. R., *Powder Technol.* **30,** 123 (1980).
5. Wall, G. C., and Brown, R. J. C., *J. Colloid Interface Sci.* **82,** 141 (1981).
6. Conner, Wm. C., unpublished results to be submitted for publication.
7. Dullien, F. A. L., and Dhawen, G.K., *J. Colloid Interface Sci.* **47,** 337 (1974).
8. Wardlow, N. C., and McKellar, M., *Powder Technol.* **29,** 127 (1981).
9. Lane, A. M., Shah, N., and Conner, Wm. C., submitted for publication.